Robust Control of an Off-Road Single-Wheel Module Using Sliding Mode Control and Fuzzy Logic Corrector*

Masood Ghasemi, David Gorsich, Vladimir Vantsevich, Lee Moradi, Jesse Paldan, Michael Cole, Jill Goryca, and Amandeep Singh

Abstract— **In this paper, the linear speed tracking control problem of a single-wheel module (SWM) operating in an off-road environment is discussed. The approach is an extension to the authors' previous work for angular speed control based on sliding mode control methodology. The linear speed tracking is performed by incorporating an adjusted reference angular speed. This reference speed is constructed utilizing a proportional control method. Further, two different approaches for tire slippage suppression are proposed. Both methods provide a corrected reference angular speed such that tracking it limits the tire slippage growth. The first method utilizes a pre-defined slippage limit, while the second method bounds the slippage by considering a range of characteristic slippages corresponding to different tire-terrain attributes. The second method is based on fuzzy logic control and specifically is designed according to Mamdani fuzzy inference system and is called the fuzzy logic corrector in this paper. The efficacy of the controlled system is evaluated through numerical simulations. It is shown that the system is able to robustly track the reference linear speed while it suppresses the tire slippage.**

I. Introduction

The technological move from conventional to individual drive wheels has opened up a new era for electric vehicles (EVs) with enhanced potential for mobility, maneuverability, and energy efficiency. This was made possible because of an agile and over-actuated powertrain, and distributed control of all individual wheels [1-3]. Simultaneously, the level of complexity of drivetrain, control and optimization has been increased, which has attracted the attention of many researchers and has led to the development of new methodologies for tire slippage control, traction control, break control, suspension control, and maneuverability control [4, 5].

Different braking slippage control algorithms based on proportional-integral (PI) control and sliding mode control were studied in [4]. Performance factors accounting for driving safety, driving comfort, control quality, and control agility of each method were evaluated through simulation and experimentation. Specifically, agile reaction, precise tire slippage tracking, chattering, and frequency band braking torque demand were compared. In [6], an MPC-based slippage control for a vehicle with all individual drive wheels was proposed. The authors in [7] developed PI- and FL-based angular speed controller for an EV with four in-wheel motors (IWMs). It was shown that the FLC exhibits a superior performance with a good response without overshoot, zero steady state error, robust disturbance rejection, and a better energy efficiency. A hierarchical LQR-based slippage control was proposed in [8]. It was shown that the design provides a better traction performance compared to a nominal sliding mode controller.

Majority of control designs including the above work rely on a pre-defined reference tire slippage and thus, do not account for varying road conditions. This is more critical in off-road applications where constant reference slippage may lead to degradation of the system performance in terms of mobility, maneuverability, agility, and energy efficiency. In on-road applications, the optimal tire slippage lies below 15%. However, in off-road applications, this range may extend to 50% of slippage or even more. Applications that are dealing with uncertain and stochastic tire-terrain attributes demand a robust and adaptive speed and slippage control approaches so as to enhance the performance of an EV with individually driven wheels.

The authors in [9] demonstrated the possibility of robust traction control for off-road electric vehicle with individual in-wheel motors. The performance of both the wheel slip and speed control approaches were illustrated and experimented on an icy surface. In a study of a commercial vehicle with mechanical drivetrain compared with a similar vehicle with individually driven wheels reported in [10], it was shown that with fully automated individual wheels drive, the traction performance as well as the maneuverability of conventional vehicle concepts can be reached or exceeded. In another work, the authors in [11] provided a control design reinforcement learning and fuzzy logic control that guarantees agile tire mobility control in the presence of drastic stochastic terrain attribute changes.

The study in this paper is motivated by research gaps for off-road application of EVs with individually driven wheels, and extends the speed and slip control concept introduced in previous paper of the authors in [12]. Specifically, a corner model of a 4x4 vehicle is considered and linear speed and slippage control solution based on sliding mode control, P-action control, and fuzzy logic control are investigated.

*Research supported by Automotive Research Center (ARC) under federal award No. W56HZV-19-2-0001 and ARC subaward No. SUBK00013996. DISTRIBUTION A. Approved for public release; distribution unlimited. (OPSEC #5818).

M. Ghasemi, V. Vantsevich, L. Moradi, and J. Paldan are with the University of Alabama at Birmingham, Birmingham, AL 35294, USA. E-mails: {mghasemi, jpaldan, vantsevi, moradi}@uab.edu.

D. Gorsich, M. Cole, J. Goryca, and A. Singh are with the U.S. Army Ground Vehicle Systems Center, Warren, MI 48397 USA. Emails: {david.j.gorsich.civ, michael.p.cole26.civ, jill.e.goryca.civ, amandeep.singh2.civ}@army.mil.

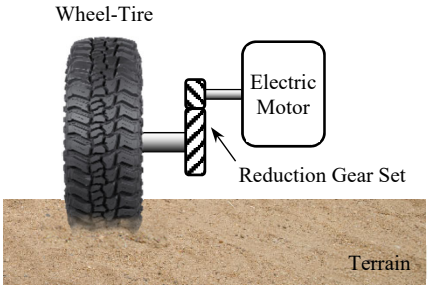

Fig. 1. The propulsion sub-system of a single wheel module.

II. Single-Wheel Module

A single-wheel module (SWM) is defined as a simulation model of a quarter of a 4x4 vehicle, which includes a single wheel-tire system, propulsion system (an electric motor and a driveline), brake, suspension, and steering. The schematic of the propulsion sub-system is shown in Fig. 1. This sub-system is powered by a DC electric motor whose generated power is transmitted through a reduction gear set to the wheel, and thus, drives the SWM forward.

The rotational dynamics of the SWM with rigid mechanical connections from the electrical motor to the wheel is given as

$$\frac{d}{dt} i_{\mathrm{m}}(t) = -\frac{R_{\mathrm{m}}}{L_{\mathrm{m}}} i_{\mathrm{m}}(t) - \frac{k_{\mathrm{emf}}}{u_{\mathrm{g}} L_{\mathrm{m}}} \omega_{\mathrm{w}}(t) + \frac{k_{\mathrm{b}}}{L_{\mathrm{m}} v_{\mathrm{b}}} u(t) + h_1(t), \tag{1}$$

$$\dot{\omega}_{\mathrm{w}}(t) = \frac{k_{\mathrm{t}}}{u_{\mathrm{g}} J_{\mathrm{eq}}} i_{\mathrm{m}}(t) - \frac{1}{J_{\mathrm{eq}}} T_{\mathrm{wl}}(t) + h_2(t), \tag{2}$$

where $i_{\mathrm{m}} \in \mathbb{R}$ is the electrical current of the motor circuit, $\omega_{\mathrm{w}} \in \mathbb{R}$ is the wheel angular speed, $u \in \mathbb{R}$ is the control input voltage, $h_1(\cdot): \mathbb{R} \to \mathbb{R}$ accounts for modeling uncertainties and matched disturbances acting on the system, $T_{\mathrm{wl}}(\cdot): \mathbb{R} \to \mathbb{R}$ is the wheel load torque, $h_2(\cdot): \mathbb{R} \to \mathbb{R}$ accounts for bearings and structural damping torques, rolling resistance, linear inertia and other modeling uncertainties as well as mismatched disturbances acting on the system, R_{m} is the resistance of the motor circuit, L_{m} is the inductance of the motor circuit, k_{emf} is the electro-motive force coefficient, k_{t} is the motor constant, u_{g} is the reduction gear ratio, J_{eq} is the equivalent rotational inertia of the rotating components of the SWM (including the rotor shaft, the gears and the wheel) calculated at the wheel side, k_{b} is the battery to pulse-width modulation (PWM) ratio, and v_{b} is the maximum battery voltage. The longitudinal dynamics is given as

$$\dot{v}_x = \frac{1}{m}(F_x(t) - R_x(t)) - g\sin\theta(t), \tag{3}$$

where $v_x \in \mathbb{R}$ is the wheel linear speed, $F_x(\cdot): \mathbb{R} \to \mathbb{R}$ is the circumferential reaction force, $R_x(\cdot): \mathbb{R} \to \mathbb{R}$ is the resistance to motion force including the rolling resistance, the drag force, and the drawbar force, g is the gravity acceleration, and $\theta \in \mathbb{R}$ is the slope of the terrain, and m is the total mass of the SWM.

Note that the rotational dynamics of (2) is coupled with the longitudinal dynamics of (3) through the tire-terrain interaction. Specifically, the wheel load torque and the circumferential force are related as

$$T_{\mathrm{wl}}(t) = r_{\mathrm{w}}^0 F_x(t), \tag{4}$$

where $r_{\mathrm{w}}^0 > 0$ is the rolling radius of the tire in driven mode, which is calculated at zero wheel torque. Further note that the circumferential force depends on the normal load, which couples the suspension dynamics (not discussed in this paper) and the longitudinal and rotational dynamics. Nonetheless, the system can be decoupled by estimating the unknown stochastic force/torque fields due to tire-terrain interactions, which will be discussed in the next section.

III. Rotational and Longitudinal Dynamics Control

Disturbances widely exist in many practical systems and could degrade system control performance, and may result in system instability. Therefore, developing a robust and effective disturbance rejection method is critical in the design process of a control system [13, 14]. In order to address the above problem, a continuous sliding mode controller coupled with the uniformly finite time exact disturbance observer (differentiator) is presented such that it ensures exact disturbance estimation and system convergence.

A. Tire-Terrain Force/Torque Field Estimation

Super-twisting and higher order sliding mode differentiators [15-17] belong to a class of disturbance observers that guarantee finite time estimation. These disturbance observers exhibit superior performance, including stronger insensitivity to external disturbances, better disturbance rejection performance, higher convergence accuracy and finite-time convergence [18-22]. Due to uncertain and stochastic nature of the tire-terrain dynamic, the higher order sliding modes differentiator class with aforementioned advantages is considered as a proper candidate in order to achieve an agile estimation and control solution. Specifically, a model-free differentiator based on the method introduced in [22], which utilizes the super-twisting higher order sliding mode observer, is utilized in this paper.

In order to estimate the unknown stochastic wheel load toque, the output of system (1)-(2) is defined as

$$y(t) \triangleq \omega_{\mathrm{w}}(t) - \frac{k_{\mathrm{t}}}{u_{\mathrm{g}} J_{\mathrm{eq}}} q_{\mathrm{m}}(t). \tag{5}$$

where $q_{\mathrm{m}} \in \mathbb{R}$ is the electrical charge of the motor circuit given as

$$q_{\mathrm{m}}(t) \triangleq \int_0^t i_{\mathrm{m}}(\tau) d\tau. \tag{6}$$

Accordingly, the wheel load torque and its time derivative are estimated as

$$\begin{cases} \xi_1(t) \triangleq \dot{y}(t) \to -\frac{1}{J_{\mathrm{eq}}} T_{\mathrm{wl}}(t) \\ \xi_2(t) \triangleq \ddot{y}(t) \to -\frac{1}{J_{\mathrm{eq}}} \dot{T}_{\mathrm{wl}}(t) \end{cases}, \tag{7}$$

where the differentiator's states, $\xi_1, \xi_2 \in \mathbb{R}$, are used in the control design.

B. Sliding Mode Control Design

Let $\omega_{\mathrm{wr}}(\cdot): \overline{\mathbb{R}}_+ \to \mathbb{R}$ be a C^2 differentiable function of time and denote the reference angular speed of the wheel whose first and second time derivatives are given. The control objective is to track the reference angular speed. Then, the error state, $e_\omega \in \mathbb{R}$, is defined as

$$e_\omega(t) \triangleq \omega_{\mathrm{w}}(t) - \omega_{\mathrm{wr}}(t),\ t \geq 0. \tag{8}$$

Let $X(t) \triangleq [i_{\mathrm{m}}(t), \omega_{\mathrm{w}}(t), \xi_1(t)]^{\mathrm{T}} \in \mathbb{R}^3$. Then, a sliding mode controller is designed to ensure the stability of the closed-loop system given as [12]

$$\begin{aligned} u(t) = &-\frac{L_{\mathrm{m}} v_{\mathrm{b}}}{k_{\mathrm{b}}}\left(K_1 - \frac{R_{\mathrm{m}}}{L_{\mathrm{m}}}\right) i_{\mathrm{m}}(t) + \frac{v_{\mathrm{b}} k_{\mathrm{emf}}}{u_{\mathrm{g}} k_{\mathrm{b}}} \omega_{\mathrm{w}}(t) \\ &-\varsigma\left(\xi_2(t) - \dot{\omega}_{\mathrm{wr}}(t) + K_1\left(\xi_1(t) - \dot{\omega}_{\mathrm{wr}}(t)\right)\right) - \frac{L_{\mathrm{m}} v_{\mathrm{b}}}{k_{\mathrm{b}}} \\ &\cdot \left(K_2 |\sigma(X,t)|^{\alpha_1} + K_3 |\sigma(X,t)|^{\alpha_2}\right) \mathrm{sign}\left(\sigma(X,t)\right), \end{aligned} \tag{9}$$

where

$$\begin{aligned} \sigma(X,t) \triangleq\ & i_{\mathrm{m}}(t) + \frac{u_{\mathrm{g}} J_{\mathrm{eq}}}{k_{\mathrm{t}}} \xi_1(t) + \frac{u_{\mathrm{g}} J_{\mathrm{eq}} K_1}{k_{\mathrm{t}}} \omega_{\mathrm{w}}(t) \\ &- \frac{u_{\mathrm{g}} J_{\mathrm{eq}}}{k_{\mathrm{t}}} \dot{\omega}_{\mathrm{wr}}(t) - \frac{u_{\mathrm{g}} J_{\mathrm{eq}} K_1}{k_{\mathrm{t}}} \omega_{\mathrm{wr}}(t), \end{aligned} \tag{10}$$

$$\varsigma \triangleq \frac{k_{\mathrm{r}} J_{\mathrm{eq}} L_{\mathrm{m}} v_{\mathrm{b}}}{k_{\mathrm{t}} k_{\mathrm{b}}}. \tag{11}$$

$K_2, K_3 > 0$ are control gains, $\alpha_1 \in [0,1), \alpha_2 \geq 1$ are constant parameters, and $\mathrm{sign}(\cdot): \mathbb{R} \to [-1,1]$ is the signum finction. The term for K_2 gain guarantees finite-time stability of the sliding surface, the term for K_3 gain ensures fast stability of the sliding surface, and the terms for K_1 gain guarantee stability of the closed-loop system on the sliding surface itself [12]. Since the reference is not published yet, readers are referred to Appendix A for further details of the design and stability analysis.

C. Linear Speed Control

Due to tire slippage, the theoretical linear speed of the wheel, $v_{\mathrm{t}}(t) \triangleq r_{\mathrm{w}}^0 \omega_{\mathrm{w}}(t)$, is not equal to its actual linear speed, $v_x(t)$. Practically, the control of the actual linear speed is deemed necessary so as to ensure that the SWM is able to accomplish timely operations. The tire slippage is a non-dimensional discrepancy measure of the theoretical and actual linear speeds of the wheel. Specifically, it is defined as

$$s_\delta(t) \triangleq \frac{v_{\mathrm{t}}(t) - v_x(t)}{\max\left(v_{\mathrm{t}}(t), v_x(t)\right)}. \tag{12}$$

To best utilize the design for rotational dynamics control while incorporating the longitudinal dynamics, the reference tire slippage, $s_{\delta \mathrm{r}} \in \mathbb{R}$ is introduced as

$$s_{\delta \mathrm{r}}(t) \triangleq \frac{r_{\mathrm{w}}^0 \omega_{\mathrm{wr}}(t) - v_x(t)}{\max\left(r_{\mathrm{w}}^0 \omega_{\mathrm{wr}}(t), v_x(t)\right)}. \tag{13}$$

Accordingly, the *adjusted* reference angular speed, $\widehat{\omega}_{\mathrm{wr}}(\cdot): \overline{\mathbb{R}}_+ \to \mathbb{R}$, is designed as

$$\widehat{\omega}_{\mathrm{wr}}(t) \triangleq \omega_{\mathrm{wr}}(t)\left(1 + K_4 s_{\delta \mathrm{r}}(t)\right),\ t \geq t_v, \tag{14}$$

where $K_4 > 0$ is a proportional control gain, and $t_v > 0$ is the switching time at which the tracking error of the linear speed, $|e_v(t_v)| \triangleq |v_x(t_v) - r_{\mathrm{w}}^0 \omega_{\mathrm{wr}}(t_v)|$, is small.

D. Slippage Suppression

The growth of the slippage may easily lead to wheel spinning and the loss of mobility. Therefore, it is desirable to maintain the slippage within certain limits. This can be achieved by correcting the error signal and thus, by limiting the control input and the power delivery to the wheel. Let

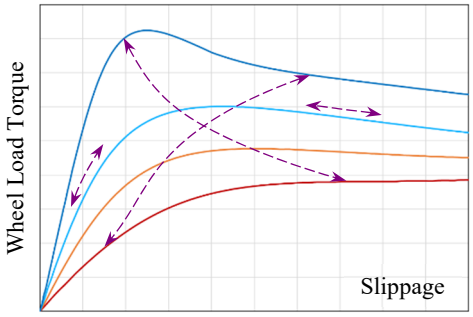

Fig. 2. Schematic of wheel load torque and tire slippage relations and their variations associated with different terrain conditions.

$\bar{\omega}_{\mathrm{wr}} \in \mathbb{R}$ denote the *corrected* reference angular speed of the wheel. Incorporating $\bar{\omega}_{\mathrm{wr}}$ in (12) yields

$$\bar{s}_\delta = \frac{|r_{\mathrm{w}}^0 \bar{\omega}_{\mathrm{wr}}(t) - v_x(t)|}{\max\left(r_{\mathrm{w}}^0 \bar{\omega}_{\mathrm{wr}}, v_x(t)\right)} > 0, \tag{15}$$

where $\bar{s}_\delta$ is the maximum allowed slippage. Solving (15) for $\bar{\omega}_{\mathrm{wr}}$ gives

$$\bar{\omega}_{\mathrm{wr}}(t) = \frac{v_x(t)}{r_{\mathrm{w}}^0}(1 - \bar{s}_\delta)^{\mathrm{sign}(-s_\delta(t))}. \tag{16}$$

The corrected reference angular speed of (16) is activated if

$$|v_x(t) - r_{\mathrm{w}}^0 \bar{\omega}_{\mathrm{wr}}(t)| \leq |v_x(t) - r_{\mathrm{w}}^0 \widehat{\omega}_{\mathrm{wr}}(t)|. \tag{17}$$

Otherwise, the adjusted reference angular speed of (14) is utilized.

Remark 1. The adjusted and corrected reference angular speeds depend of the wheel linear speed whose time derivatives can be written using the dynamics model of the SWM and the estimated circumferential force and its time derivative. However, due to great uncertainties related to resisting to motion forces, $R_x(\cdot)$, and the terrain slope, θ, in (3), the above model-based approach is not feasible. Instead, the model free differentiator (see Section III.A) is utilized to robustly estimate the time derivatives of $\widehat{\omega}_{\mathrm{wr}}$ and $\bar{\omega}_{\mathrm{wr}}$.

IV. Fuzzy Logic Corrector

The environment at which off-road vehicles are operating is characterized by its wild dynamics nature, that is attributes like height profile, soil composition, soil grain size, moisture content, vegetation, and deformability are highly varied from one region to another. Employing control strategies that rely on constant specification of a terrain attributes may lead to low efficiency due to low mobility or agility performance.

In order to address the above problem, a strategy based on fuzzy logic control is adopted. Specifically, a fuzzy logic controller provides a corrected reference angular speed of the wheel such that tracking it ensures slippage suppression in accordance with any different environmental conditions. The fuzzy logic controller is called the fuzzy logic corrector in this paper to emphasize on its role when it is superimposed with the sliding mode controller discussed in Section III.B. The design of the fuzzy logic corrector is based on Mamdani fuzzy inference system [23]. The details are given as follows.

The inputs to the fuzzy logic corrector are selected such that they provide sufficient and minimum information required for slippage suppression purpose. Analyzing the

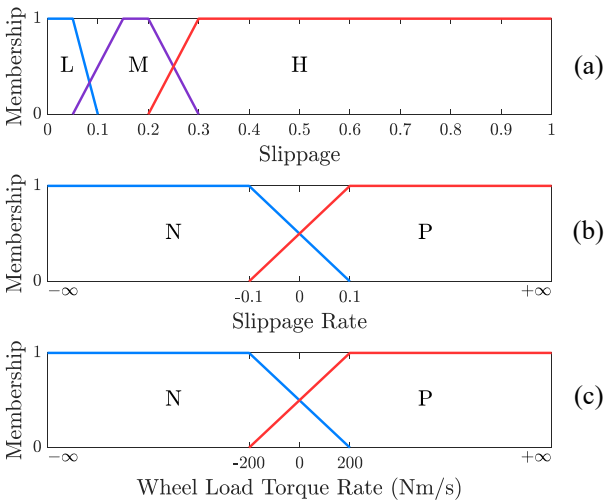

Fig. 3. The membership functions of the inputs to the fuzzy logic corrector, a) slippage, b) slippage rate, c) wheel load torque rate.

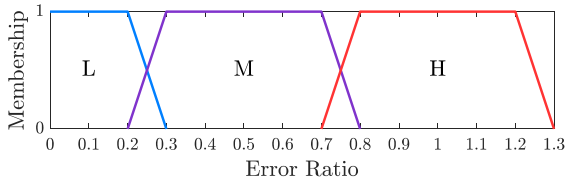

Fig. 4. The membership function of the output of the fuzzy logic corrector.

diagram of wheel load torque-tire slippage illustrated in Fig. 2 suggests that such candidate inputs are 1) the tire slippage, $|s_\delta(t)|$, 2) the rate of changes of the tire slippage, $\text{sign}\big(s_\delta(t)\big)\,\dot{s}_\delta(t)$, and 3) the rate of changes of the wheel load torque, $\text{sign}\big(s_\delta(t)\big)\,\dot{T}_{\text{wl}}(t)$.

The optimal dynamic behavior of the wheel specified with respect to maximum mobility or energy efficiency defines a desired slippage range of the tire-terrain interaction. The upper bound of this range is identified as a characteristic or critical slippage. Due to stochastic and dynamic nature of a terrain, a characteristic slippage is not constant and heavily depends on the tire-terrain attributes. Therefore, instead of having a single valued characteristic slippage, a range is defined. Such characteristic can be reflected in the membership functions definition. Specifically, the tire slippage membership functions as shown in Fig. 3.a. The ranges are labeled as L (low), M (medium), and H (high). Further, the membership functions of the slippage rate and the wheel load torque rate are depicted in Fig. 3.b and Fig. 3.c, respectively. Their ranges are labeled as N (negative) and P (positive).

The output of the fuzzy logic corrector is the corrected reference angular speed. Nonetheless, the range of desired speeds may vary depending on a mission. Further, the corrected angular speed should reflect upon the range of characteristic slippages. In order to address the above requirements, first, the upper bound of the reference angular speed is defined as

$$\omega_{\text{wr1}}(t) \triangleq \frac{v_x(t)}{r_{\text{w}}^0}(1-\max\{s_{\delta\text{c}}\})^{\text{sign}(-s_\delta(t))}, \qquad (18)$$

TABLE 1. THE LINGUISTIC RULES OF THE FUZZY LOGIC CORRECTOR.

Rules	**Inputs**			**Output**
#	$\lvert s_\delta\rvert$	$\text{sign}(s_\delta)\dot{s}_\delta$	$\text{sign}(s_\delta)\dot{T}_{\text{w}}$	e_δ
1	L	–	–	H
2	M	P	P	M
3	M	N	N	M
4	M	P	N	L
5	M	N	P	H
6	H	–	–	L

where $\omega_{\text{wr1}} \in \mathbb{R}$, and $s_{\delta\text{c}} \in (0,1)$ is the characteristic slippage. For linear speed tracking, the angular speed should deviate from the reference angular speed. The lower bound for such a deviation is defined considering the minimum characteristic slippage. Accordingly, a secondary bound for the reference angular speed is defined as

$$\omega_{\text{wr2}}(t) \triangleq \omega_{\text{wr}}(t)(1-\min\{s_{\delta\text{c}}\})^{\text{sign}(-s_\delta(t))}, \qquad (19)$$

where $\omega_{\text{wr2}} \in \mathbb{R}$.

Next, an error ratio, $e_\delta \in (0,1]$, is defined as

$$e_\delta(t) \triangleq \frac{\bar{\omega}_{\text{wr}}(t)r_{\text{w}}^0 - v_x(t)}{\omega_{\text{wrb}}(t)r_{\text{w}}^0 - v_x(t)}. \qquad (20)$$

where $\omega_{\text{wrb}} \in \mathbb{R}$, is a reference angular speed that determines the upper bound of the slippages. Specifically, $\omega_{\text{wrb}}(t) = \omega_{\text{wr1}}(t)$ if

$$|\omega_{\text{wr1}}(t)r_{\text{w}}^0 - v_x(t)| > |\omega_{\text{wr2}}(t)r_{\text{w}}^0 - v_x(t)|, \qquad (21)$$

Otherwise, $\omega_{\text{wrb}}(t) = \omega_{\text{wr2}}(t)$. The condition (21) is always satisfied except when the tracking error becomes small. Accordingly, the corrected reference angular speed is calculated as

$$\bar{\omega}_{\text{wr}}(t) = \frac{v_x(t)}{r_{\text{w}}^0} + e_\delta(t)\left(\omega_{\text{wrb}}(t) - \frac{v_x(t)}{r_{\text{w}}^0}\right) \qquad (22)$$

Let the output of the fuzzy logic corrector be the error ratio given by (20). Three different ranges for error ratio are identified as L (low), M (medium), and H (high). Accordingly, its membership function is defined as depicted in Fig. 4. Note that the range of the error ratio is extended to 1.3 such that the centroid of H-region is at 1.

Finally the linguistic rules are obtained by considering different scenarios of the temporal changes of the wheel load torque versus tire slippage (Fig. 2) and assigning proper strategies to ensure slippage is suppressed accordingly. Such linguistic rules are listed in Table 1. The inputs are combined using AND logical statements. Note that the first and the sixth rules only consider slippage amplitude and do not care about other inputs.

V. SIMULATION

The important closed-loop system parameter values are listed in Table 2. For the simulation, stochastic terrain profiles representing meadow and snow types are considered. The characteristic parameters and height profiles of such terrains are generated based on the method introduced in [24]. It is assumed that the SWM experiences a terrain transition from meadow to snow starting at time $t = 2$ s for 50 ms. The stochastic peak friction coefficients of the meadow and snow terrains are shown in Fig. 5. Further, the reference angular speed of the SWM is given by

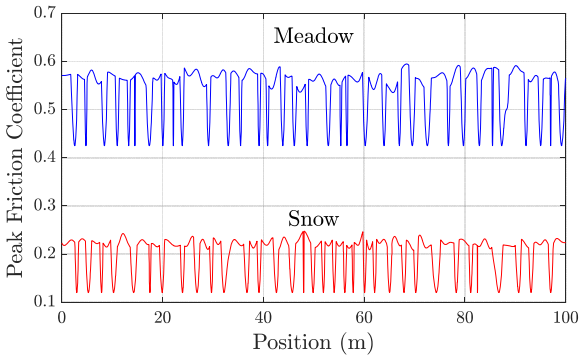

Fig. 5. The stochastic peak friction coefficient for meadow and snow terrains [24].

TABLE 2. THE PARAMETERS OF THE SWM CLOSED-LOOP SYSTEM

Parameter	Value	Unit	Parameter	Value	Unit
m	1457	kg	r_{w}^{0}	0.491	m
J_{eq}	30.42	kgm^2	K_1	80	–
u_{g}	0.1028	–	K_2	15	–
L_{m}	1.2	mH	K_3	1	–
R_{m}	0.25	Ω	K_4	25	–
$k_{\mathrm{t}} = k_{\mathrm{emf}}$	2	–	α_1	0	–
k_{b}	120	V	α_2	1.5	–

$$w_{\mathrm{wr}}(t) = \frac{1}{r_{\mathrm{w}}^{0}}\left(10 + \sin\left(t - \frac{\pi}{6}\right)\right), \quad \text{(rad/s)} \qquad (23)$$

Two simulations are performed with an objective of linear speed tracking, that is $v_x(t) \to r_{\mathrm{w}}^{0} w_{\mathrm{wr}}(t)$. In the first simulation, the slippage suppression is done based on the corrected reference angular speed of (16) for which $\bar{s}_\delta = 0.2$. The results are depicted in Figs 6-8. Specifically, the time history of the sliding mode control input is shown in Fig. 6, the time history of the SWM theoretical and actual linear speeds are depicted in Fig. 7, and the time history of the tire slippage is shown in Fig. 8. The closed-loop system is able to affectively track reference linear speed by tracking the corrected reference speed ($t < 3.3$ s) and the adjusted reference speed ($t > 3.3$ s) while suppressing slippage to 20%. At the time of terrain transition, the system exhibits an overshoot, which results in about 4% slippage growth. However, it is suppressed shortly after.

For the second simulation, the fuzzy logic corrector is utilized and the corrected reference angular speed is calculated using (22). Further, the minimum and maximum characteristic slippages are assumed to be 0.15 and 0.5, respectively. The results are depicted in Figs. 9-12. Specifically, the time history of the sliding mode control input is shown in Fig. 9, the time history of the output of the fuzzy logic corrector is depicted in Fig. 10, the time history of the SWM theoretical and actual linear speeds are depicted in Fig. 11, and the time history of the tire slippage is shown in Fig. 12. The closed-loop system is able to affectively track reference linear speed by tracking the corrected reference speed ($t < 3.0$ s) and the adjusted reference speed ($t > 3.0$ s). The tire slippage is suppressed to 30% in the initial phase. However, it is kept as low as 10% after the terrain transition. Unlike the first simulation, the closed-loop system does not exhibit any overshoot at the time of terrain transition. Further, due to awareness of the varied

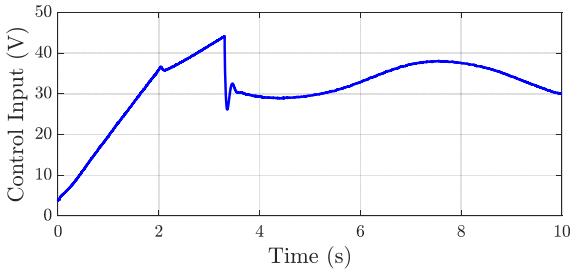

Fig. 6. The time history of the sliding mode control input.

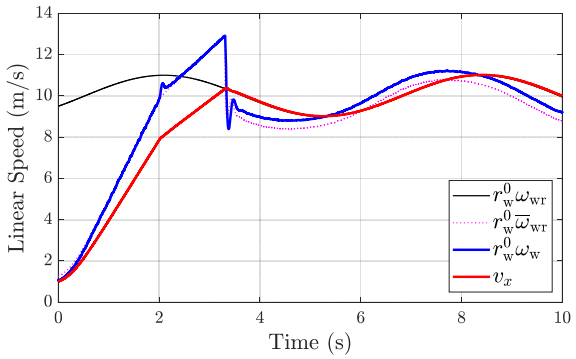

Fig. 7. The time history of the reference, theoretical, and actual linear speeds of the SWM.

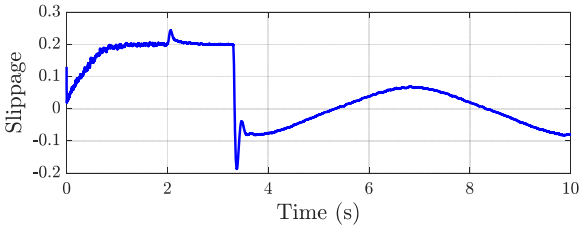

Fig. 8. The time history of the tire slippage.

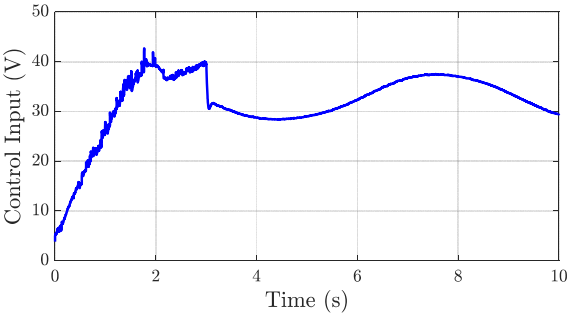

Fig. 9. The time history of the sliding mode control input.

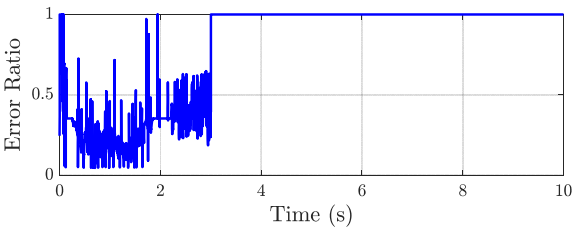

Fig. 10. The time history of the output of the fuzzy logic corrector.

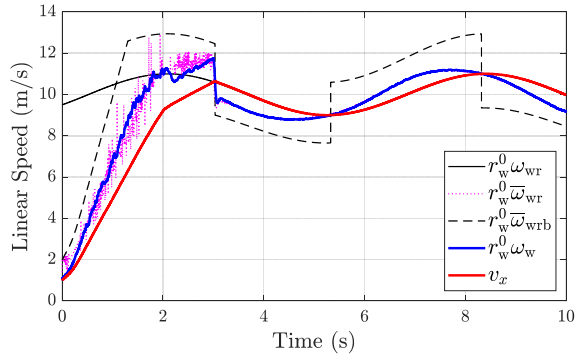

Fig. 11. The time history of the reference, theoretical, and actual linear speeds of the SWM.

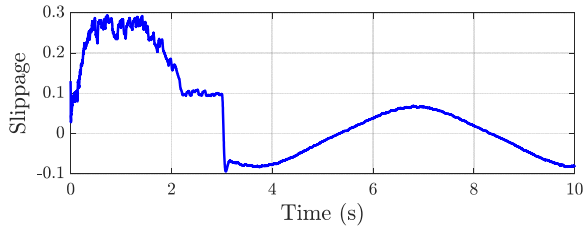

Fig. 12. The time history of the tire slippage.

characteristic slippage, the superimposed control solution of the sliding mode controller and the fuzzy logic corrector was able to reach the reference linear speed faster compared to the case of the first solution.

VI. Conclusion

In this paper, the linear speed tracking control problem of a SWM operating in an off-road environment was discussed. The approach combined a sliding mode controller capable of angular speed tracking with an adjusted reference angular speed constructed based on a proportional control method. Further, two different approaches for tire slippage suppression were discussed. These methods utilized a corrected reference angular speed such that tracking it limits the tire slippage growth. The first method utilized a pre-defined slippage limit, while the second method considered a range of slippages. The second method was referred to as the fuzzy logic corrector. Next, the efficacy of the controlled system were evaluated through numerical simulations. It was shown that the system was able to robustly track the reference linear speed while it suppressed the tire slippage. The fuzzy logic corrector was able to perform a better slippage control by suppressing the slippage at different levels depending on terrain attributes. Nonetheless, the first slippage suppression method provided a constant suppression level while exhibited an overshoot at the time of a terrain transition.

Appendix A. Sliding Mode Control Design

Let $\omega_{wr}(\cdot)\colon \bar{\mathbb{R}}_+ \to \mathbb{R}$ be a C^2 differentiable function of time and denote the reference angular speed of the wheel whose first and second time derivatives are given. The control objective is to track the reference angular speed. Then, the error state, $e_\omega \in \mathbb{R}$, is defined as

$$e_\omega(t) \triangleq \omega_w(t) - \omega_{wr}(t),\ t \geq 0 \tag{A.1}$$

Next, consider a scalar function $\sigma(\cdot,\cdot)\colon \mathbb{R}^3 \times \mathbb{R} \to \mathbb{R}$ defined as

$$\sigma(X,t) \triangleq i_m(t) + \frac{u_g J_{eq}}{k_t}\xi_1(t) + \frac{u_g J_{eq} K_1}{k_t}\omega_w(t) - \frac{u_g J_{eq}}{k_t}\dot{\omega}_{wr}(t) - \frac{u_g J_{eq} K_1}{k_t}\omega_{wr}(t), \tag{A.2}$$

where $X(t) \triangleq [i_m(t), \omega_w(t), \xi_1(t)]^T \in \mathbb{R}^3$, and $K_1 > 0$. Accordingly, the sliding surface is defined as the null space of $\sigma(\cdot,\cdot)$ as

$$\mathcal{S} \triangleq \{(X,t) \in \mathbb{R}^3 \times \mathbb{R} : \sigma(X,t) = 0\}. \tag{A.3}$$

The time derivative of $\sigma(\cdot,\cdot)$ along the trajectories of (1)-(2) yields

$$\begin{aligned}\frac{d}{dt}\sigma(X,t) &= \frac{d}{dt}i_m(t) + \frac{u_g J_{eq}}{k_t}\dot{\xi}_1(t) + \frac{u_g J_{eq} K_1}{k_t}\dot{\omega}_w(t) - \frac{u_g J_{eq}}{k_t}\ddot{\omega}_{wr}(t) - \frac{u_g J_{eq} K_1}{k_t}\dot{\omega}_{wr}(t)\\ &= \left(K_1 - \frac{R_m}{L_m}\right)i_m(t) - \frac{k_{emf}}{u_g L_m}\omega_w(t) + \frac{k_b}{L_m v_b}u(t) + \frac{u_g J_{eq}}{k_t}\xi_2(t) + \frac{u_g J_{eq} K_1}{k_t}\xi_1(t) - \frac{u_g J_{eq}}{k_t}\ddot{\omega}_{wr}(t) - \frac{u_g J_{eq} K_1}{k_t}\dot{\omega}_{wr}(t).\end{aligned} \tag{A.4}$$

In the above derivation, the estimates $T_{wl}(t) \approx -J_{eq}\xi_1(t)$ and $\dot{\omega}_w(t) \approx \xi_1(t) + \frac{k_t}{u_{rg} J_{eq}} i_m(t)$ are utilized. Finally, the SMC is designed to ensure finite-time stability of the sliding surface, $\mathcal{S}$. Specifically, the controller is given as

$$\begin{aligned}u(t) = &-\frac{L_m v_b}{k_b}\left(K_1 - \frac{R_m}{L_m}\right)i_m(t) + \frac{v_b k_{emf}}{u_g k_b}\omega_w(t)\\ &-\varsigma\left(\xi_2(t) - \ddot{\omega}_{wr}(t) + K_1\left(\xi_1(t) - \dot{\omega}_{wr}(t)\right)\right) - \frac{L_m v_b}{k_b}\\ &\cdot\left(K_2|\sigma(X,t)|^{\alpha_1} + K_3|\sigma(X,t)|^{\alpha_2}\right)\mathrm{sign}\left(\sigma(X,t)\right),\end{aligned} \tag{A.5}$$

where $K_2, K_3 > 0$ are control gains, $\alpha_1 \in [0,1), \alpha_2 \geq 1$ are constant parameters, and

$$\varsigma \triangleq \frac{k_r J_{eq} L_m v_b}{k_t k_b}. \tag{A.6}$$

The stability analysis of the closed-loop system is performed in two steps: 1) the stability analysis of the sliding surface (A.3) and 2) the stability analysis of the reduced order dynamics on the sliding surface. First, consider a candidate Lyapunov function as $V(\sigma) \triangleq \frac{1}{2}\sigma^2$ and note that $V(0) = 0$ and $V(\sigma) > 0$, $\sigma \neq 0$. The time derivative of $V(\cdot)$ along the trajectories of the closed-loop system yields

$$\begin{aligned}\dot{V}(\sigma) &= \sigma\dot{\sigma}\\ &= \sigma\Bigg(\left(K_1 - \frac{R_m}{L_m}\right)i_m(t) - \frac{k_{emf}}{u_g L_m}\omega_w(t) + \frac{k_b}{L_m v_b}u(t) + \frac{u_g J_{eq}}{k_t}\xi_2(t) + \frac{u_g J_{eq} K_1}{k_t}\xi_1(t) - \frac{u_g J_{eq}}{k_t}\ddot{\omega}_{wr}(t)\end{aligned}$$

$$-\frac{u_{\mathrm{g}}J_{\mathrm{eq}}K_1}{k_{\mathrm{t}}}\dot{\omega}_{\mathrm{wr}}(t)+h_1(t)+\frac{u_{\mathrm{g}}J_{\mathrm{eq}}K_1}{k_{\mathrm{t}}}h_2(t)\Bigg)$$

$$=\sigma\Big(-(K_2|\sigma(X,t)|^{\alpha_1}+K_3|\sigma(X,t)|^{\alpha_2})\,\mathrm{sign}\big(\sigma(X,t)\big)+h_1(t)+\big(u_{\mathrm{g}}J_{\mathrm{eq}}K_1/k_{\mathrm{t}}\big)h_2(t)\Big). \quad (A.7)$$

Let

$$K_2 \triangleq \lambda+\|h_1(t)\|_\infty+\frac{u_{\mathrm{g}}J_{\mathrm{eq}}K_1}{k_{\mathrm{t}}}\|h_2(t)\|_\infty, \quad (A.8)$$

where $\lambda>0$. Then,

$$\begin{aligned}\dot{V}(\sigma)&\le-|\sigma|(\lambda|\sigma(X,t)|^{\alpha_1}+K_3|\sigma(X,t)|^{\alpha_2})\\&\le-\lambda|\sigma(X,t)|^{\alpha_1+1}+K_3|\sigma(X,t)|^{\alpha_2+1}\\&\le-2^{\frac{\alpha_1+1}{2}}\lambda V^{\frac{\alpha_1+1}{2}}(\sigma).\end{aligned} \quad (A.9)$$

Note that $\frac{\alpha_1+1}{2}\in(0.5,1)$. Thus, According to Theorem 4.17 [25], the sliding surface (A.3) is finite-time stable.

Next, the stability of the reduced order dynamics on the sliding surface is analyzed. Let $t_{\mathrm{c}}^*>0$ be the upper estimate of the settling time of the sliding surface. Then, for any $t>t_{\mathrm{c}}^*$, the reduced order dynamics on the sliding surface (A.3) is obtained as

$$\begin{aligned}\sigma(X,t)&=i_{\mathrm{m}}(t)+\frac{u_{\mathrm{g}}J_{\mathrm{eq}}}{k_{\mathrm{t}}}\left(\dot{\omega}_w(t)-\frac{k_t}{u_{\mathrm{g}}J_{eq}}i_m(t)\right)\\&\quad+\frac{u_{\mathrm{g}}J_{\mathrm{eq}}}{k_{\mathrm{t}}}\big(K_1\omega_{\mathrm{w}}(t)-\dot{\omega}_{\mathrm{wr}}(t)-K_1\omega_{\mathrm{wr}}(t)\big)\\&=\frac{u_{\mathrm{g}}J_{\mathrm{eq}}}{k_{\mathrm{t}}}\big(\dot{e}_\omega(t)+K_1e_\omega(t)\big)\\&=0.\end{aligned} \quad (A.10)$$

The dynamics of (A.10) is globally exponentially stable for $K_1>0$, which completes the proof of stability.

REFERENCES

[1] H. Yang, C. Liu, J. Shi, and G. Zheng, "Development and Control of Four-Wheel Independent Driving and Modular Steering Electric Vehicles for Improved Maneuverability Limits," SAE Technical Paper, 2019.

[2] Y. Sun, M. Li, and C. Liao, "Analysis of Wheel Hub Motor Drive Application in Electric Vehicles," *MATEC Web Conf.,* vol. 100, p. 01004, 2017.

[3] M. S. Jneid, P. Harth, and P. Ficzere, "In-Wheel-Motor Electric Vehicles and Their Associated Drivetrains," *International Journal for Traffic and Transport Engineering,* vol. 10, no. 4, 2020.

[4] D. Savitski *et al.*, "Wheel Slip Control for the Electric Vehicle With In-Wheel Motors: Variable Structure and Sliding Mode Methods," *IEEE Transactions on Industrial Electronics,* vol. 67, no. 10, pp. 8535-8544, 2020.

[5] H. Wu, L. Zheng, and Y. Li, "Coupling effects in hub motor and optimization for active suspension system to improve the vehicle and the motor performance," *Journal of Sound and Vibration,* vol. 482, p. 115426, 2020.

[6] Y. Ma, J. Zhao, H. Zhao, C. Lu, and H. Chen, "MPC-Based Slip Ratio Control for Electric Vehicle Considering Road Roughness," *IEEE Access,* vol. 7, pp. 52405-52413, 2019.

[7] A. Ghezouani, B. Gasbaoui, N. Nair, O. Abdelkhalek, and J. Ghouili, "Comparative study of pi and fuzzy logic based speed controllers of an EV with four in-wheel induction motors drive," *Journal of Automation Mobile Robotics and Intelligent Systems,* vol. 12, no. 3, pp. 43-54, 2018.

[8] B. M. Nguyen, S. Hara, H. Fujimoto, and Y. Hori, "Slip control for IWM vehicles based on hierarchical LQR," *Control Engineering Practice,* vol. 93, p. 104179, 2019.

[9] D. Savitski *et al.*, "Improvement of traction performance and off-road mobility for a vehicle with four individual electric motors: Driving over icy road," *Journal of Terramechanics,* vol. 69, pp. 33-43, 2017.

[10] J. Kneissl, A. Lion, F. Breuer, P. Wagner, and T. Ille, "Study on the traction potential and manoeuvrability of wheel-individually driven commercial vehicle concepts," *Vehicle System Dynamics,* pp. 1-20, 2020.

[11] V. Vantsevich, D. Gorsich, A. Lozynskyy, L. Demkiv, T. Borovets, and S. Klos, "Agile Tyre Mobility: Observation and Control in Severe Terrain Environments," in *Advanced Technologies for Security Applications*: Springer, 2020, pp. 247-258.

[12] M. Ghasemi, V. V. Vantsevich, D. J. Gorsich, and L. Moradi, "Robust Control Design for a Single-Wheel Module Operating in an Off-Road Terrain with Uncertain and Stochastic Attributes," in *Modeling, Estimation and Control Conference*, 2021, pp. 1-8.

[13] L. Guo and S. Cao, "Anti-disturbance control theory for systems with multiple disturbances: A survey," *ISA Transactions,* vol. 53, no. 4, pp. 846-849, 2014.

[14] W. Chen, J. Yang, L. Guo, and S. Li, "Disturbance-Observer-Based Control and Related Methods—An Overview," *IEEE Transactions on Industrial Electronics,* vol. 63, no. 2, pp. 1083-1095, 2016.

[15] A. Levant, "Robust exact differentiation via sliding mode technique," *Automatica,* vol. 34, no. 3, pp. 379-384, 1998.

[16] Y. B. Shtessel, I. A. Shkolnikov, and A. Levant, "Smooth second-order sliding modes: Missile guidance application," *Automatica,* vol. 43, no. 8, pp. 1470-1476, 2007.

[17] A. Levant, "Higher-order sliding modes, differentiation and output-feedback control," *International Journal of Control,* vol. 76, no. 9-10, pp. 924-941, 2003.

[18] J. Hu, Z. Wang, H. Dong, and H. Gao, "Recent Advances on Recursive Filtering and Sliding Mode Design for Networked Nonlinear Stochastic Systems: A Survey," *Mathematical Problems in Engineering,* vol. 2013, p. 646059, 2013.

[19] J. Yang, S. Li, J. Su, and X. Yu, "Continuous nonsingular terminal sliding mode control for systems with mismatched disturbances," *Automatica,* vol. 49, no. 7, pp. 2287-2291, 2013.

[20] A. Ferreira de Loza, E. Punta, L. Fridman, G. Bartolini, and S. Delprat, "Nested backward compensation of unmatched perturbations via HOSM observation," *Journal of the Franklin Institute,* vol. 351, no. 5, pp. 2397-2410, 2014.

[21] Y. Shtessel, P. Yu, S. S. Mehta, and C. L. Pasiliao, "Air breathing hypersonic missile continuous higher order sliding mode control for maximum target penetration," in *2014 13th International Workshop on Variable Structure Systems (VSS)*, 2014, pp. 1-6.

[22] M. Basin, P. Yu, and Y. Shtessel, "Finite- and fixed-time differentiators utilising HOSM techniques," *IET Control Theory & Applications,* vol. 11, no. 8, pp. 1144-1152, 2017.

[23] E. H. Mamdani and S. Assilian, "An experiment in linguistic synthesis with a fuzzy logic controller," *International Journal of Man-Machine Studies,* vol. 7, no. 1, pp. 1-13, 1975.

[24] J. P. Gray, V. V. Vantsevich, A. F. Opeiko, and G. R. Hudas, "A Method for Unmanned Ground Wheeled Vehicle Mobility Estimation in Stochastic Terrain Conditions," in *Proc. of the 7th Americas Regional Conference of the ISTVS, Tampa, Florida, USA*, 2013.

[25] W. M. Haddad and V. Chellaboina, *Nonlinear dynamical systems and control: a Lyapunov-based approach*. Princeton: Princeton University Press (in English), 2008.